ChemComm

Accepted Manuscript

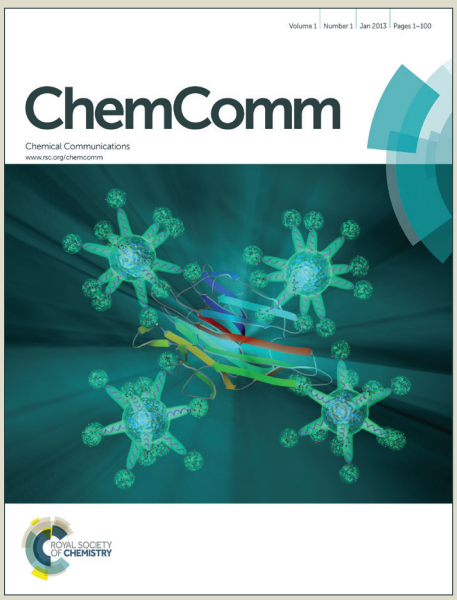

ROYAL SOCIETY OF CHEMISTRY

www.rsc.org/chemcomm

Journal Name

RSCPublishing

COMMUNICATION

Mechanochemical Lithiation of Layered Polysilane

Cite this: DOI: 10.1039/x0xx00000x

Masataka Ohashi,[a,] Hideyuki Nakano,[a, b] Tetsuya Morishita,[c] Michelle J. S. Spencer,[d] Yuka Ikemoto,[e] Chihiro Yogi,[f] and Toshiaki Ohta[f]

Received 00th January 2012,
Accepted 00th January 2012

DOI: 10.1039/x0xx00000x

www.rsc.org/

Lithiated polysilane was synthesized by the mechanochemical reaction of layered polysilane and metallic lithium. The resulting dark green powder formed Si–Li bond on the surface and demonstrated electroconductivity.

Silicon is one of the essential elements in the field of materials science, because it is applied to various functional materials, such as semiconductors, polymers, and glasses. Also, in recent years, Si has attracted attention as a promising candidate for the anode of the Li-ion battery because theoretically its specific capacity is ten times higher than commercial graphite.[1, 2] Although use of a silicon anode can realize higher energy Li-ion batteries, significant volume changes of the electrode during the reaction of Si and Li can result in loss of storage capacity because of the fracture of active silicon particles and unstable solid electrolyte interphase (SEI) growth.[2] Therefore, development of new silicon anodes and investigations into the chemistry of Si–Li composites and alloys have been undertaken to realize high capacity silicon anodes for next generation Li-ion batteries.[3, 4]

Recently, nanometer-thick materials, such as oxides[5], niobates[6], chalcogenides[7], phosphates[8], and graphene[9, 10], and their stacked compounds have attracted considerable attention due to their potential applications as catalysts, sensors, and electronic devices. We have successfully synthesized silicon nanosheets (Si-NSs) by chemical exfoliation of calcium silicide ($CaSi_2$).[11, 12] Si-NSs consisted of a monoatomic layer of silicon with a hexagonal crystal structure; the surface of the monoatomic layers was capped with hydrogen (Fig. 1a). Si-NSs are easily and strongly stacked due to van der Waals attraction and form layered polysilane (Si_6H_6), which is a graphite-like layered compound (Fig. 1b).[13] Si_6H_6 can serve as an alternative material for bulk silicon because it has a Si framework like a bulk silicon (111) plane and contains few oxygen atoms in the framework.

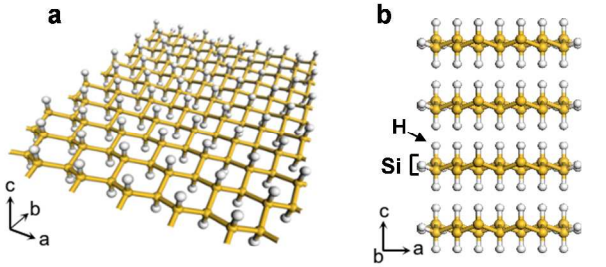

Fig. 1 Schematic images of (a) Silicon nanosheet (Si-NS) and (b) layered polysilane (Si_6H_6)

Si_6H_6 shows various functions by chemical modification of the surface Si–H groups.[14] In fact, we have reported chemical modification of Si_6H_6 using Grignard reagents or alkyl-amine reagents.[15, 16] The resulting organic modified Si_6H_6s are soluble in several organic solvents as a monolayere nanosheet and shows characteristic properties such as photo current generation and self-assembly behavior.

[a] Toyota Central R&D Laboratories, Inc., Nagakute, Aichi 480-1192 Japan. E-mail: m-ohashi@mosk.tytlabs.co.jp

[b] Japan Science and Technology Agency, PRESTO, Kawaguchi, Saitama 332-0012 Japan

[c] Nanosystem Research Institute, National Institute of Advanced Industrial Science and Technology (AIST), Central 2, 1-1-1 Umezono, Tsukuba, Ibaraki 305-8568 Japan

[d] School of Applied Sciences, RMIT University, GPO Box 2476, Melbourne, Victoria 3001 Australia

[e] SPring-8 Japan Synchrotron Radiation Research Institute (JASRI), 1-1-1 Kouto, Sayo, Hyogo 679-5198 Japan

[f] SR Center, Ritsumeikan University, 1-1-1 Noji-Higashi, Kusatsu, Shiga 525-8577 Japan

† Electronic Supplementary Information (ESI) available: Experimental and characterization details, photograph, XRD, IR, SEM, vibrational density of state and XANES of lithiated polysilane. See DOI: 10.

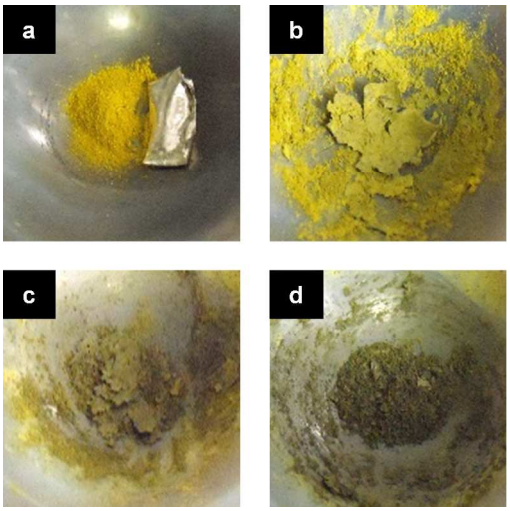

Fig. 2 Schematic representation of the mechanochemical reaction of Si_6H_6 and Li: (a) before milling, (b) 5 min, (c) 15 min, and (d) 30 min

The advantage of Si_6H_6 is the presence of highly reactive Si–H groups on the surface and between the layers. Therefore, we designed densely lithiated Si_6H_6 by the substitution of Si–H groups with Li. The lithiation of Si_6H_6 can increase the potential applications. For example, lithiated Si_6H_6 is expected to be used as a Li-ion battery anode[17] and may be a useful precursor for organic modifications. Furthermore, improving the conductivity of Si_6H_6 may be possible because of changes in the electron structure of the Si framework.

Most Si–Li composites and alloys can be prepared by electrochemical or co-melting strategies. The electrochemical lithiation of bulk silicon is a useful method to prepare Si–Li composites under mild conditions and has been thoroughly investigated as an electrode reaction of a Li-ion battery.[18] The co-melting synthesis method is also used to prepare some Li alloys by utilizing the low melting temperature of Li.[19] However, neither method is applicable to the reaction of Si_6H_6 and Li for the following reasons. The highly reactive surface of the Si-NS reacts easily with oxygen or the electrolyte and causes oxidation or decomposition of Si-NS. Furthermore, Si_6H_6 does not melt without structural deterioration. Notably, no composite can obtain even the solid–liquid phase reaction of Si_6H_6 and melted Li because phase separation between Si_6H_6 and melted Li depends on the high surface tension of melted Li.

In this study, we focused on the mechanochemical solid-phase reaction between the highly reactive Si–H groups in Si_6H_6 and Li. Homogeneous composites were formed by manually grinding Si_6H_6 and Li at room temperature and normal pressure under argon atmosphere. The obtained composites were identified by several spectroscopic and conductive measurements.

Si_6H_6 was prepared according to the method described by Yamanaka et al.[20] $CaSi_2$ was stirred in concentrated HCl at −30 °C for 7 days. The obtained Si_6H_6 was rinsed with HCl and dilute HF solution and then vacuum dried at room temperature. Si_6H_6/nLi composites were prepared by a mechanochemical solid-phase reaction. In a typical synthesis, Si_6H_6 (0.15 g, 5.2 mmol of Si–H unit) and Li (17.9 mg for n = 3, or 35.8 mg for n = 6) were placed in a mortar and milled using a pestle at room temperature under argon

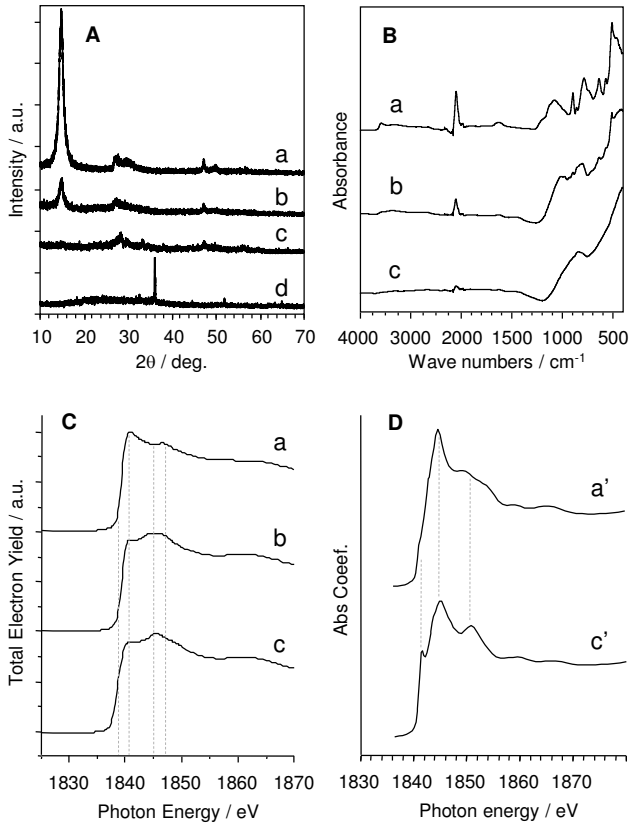

Fig. 3 X-ray diffraction patterns (A), FTIR spectra (B), and Si K-edge XANES spectra (C) of (a) Si_6H_6, (b) Si_6H_6/3Li, (c) Si_6H_6/6Li, and (d) Li. (D) Theoretical XANES spectra of (a') Si–H and (c') Si–Li structural models simulated by the FEFF program.

atmosphere. Before milling, Si_6H_6 and Li were a light yellow powder and a silver metallic thin plate, respectively (Fig. 2a). After milling for 5 min, a greenish yellow powder and a ripped fragment of Li were observed (Fig. 2b). Over the next 15 min, the color changed from greenish yellow to faded green (Fig. 2c). Finally, after 30 min of milling, the Li fragments had disappeared completely, and a dark green powder was obtained (Fig. 2d). The obtained composites were yellow to dark green, depending on the Li content (Fig. S1).

X-ray diffraction (XRD) measurements were performed on Si_6H_6 and Si_6H_6/nLi to investigate the structural changes due to the mechanochemical reaction (Fig. 3A). The diffraction peaks of Si_6H_6 can be indexed on the basis of a hexagonal unit cell with a = 0.383 nm and c = 0.598 nm, which is consistent with previous data.[13] The diffraction peaks attributed to the layered structure ((001) and (002) planes at 2θ = 14.8° and 29.9°) and the crystal structure of the Si framework ((100) and (110) planes at 2θ = 27.1° and 47.2°) changed depending on the additive amount of Li. In addition, no diffraction peak attributing to the Li metal was observed in any composite.

The diffraction peaks of (001) and (002) planes decreased dramatically and disappeared completely at Si_6H_6/6Li. The diffraction peak of (110) plane also decreased and the diffraction peak of (100) plane shifted slightly to a lower diffraction angle (or high d value). To investigate the effect of mechanical shearing for the crystal structure of Si_6H_6, mechanical milling of Si_6H_6 without Li was performed under the same conditions. The milled Si_6H_6 maintained a typical XRD pattern for the Si_6H_6, although the intensity of the (001) and (002) plane diffraction peaks decreased

slightly after milling (Fig. S2). These results indicate that the obtained Si–Li composites were formed by the reaction of Si_6H_6 and Li and are not simply a mixture of Si_6H_6 and Li. In addition, the mechanical milling of Si_6H_6 and Li resulted in the distortion of the Si framework and collapse of the layered structure. SEM images of before and after the lithiation of Si_6H_6 clearly suggested that the plate-like shapes of Si_6H_6, which resulted from the stacking of the layers, were completely destroyed by the milling process. In addition, aggregates of the lithiated layer were observed as atypical particles (Fig. S3).

To elucidate the chemical reaction between Si_6H_6 and Li, Fourier transform infrared (FTIR) spectra of Si_6H_6 and Si_6H_6/*n*Li were measured using an attenuated total reflection (ATR) unit (Fig. 3B). Si_6H_6 exhibited Si–OH (3592 cm^{-1}), Si–H (894 and 2098 cm^{-1}), Si–O–Si (1023 cm^{-1}), and Si–Si (500–800 cm^{-1}) stretching peaks. The observed Si–OH and S–O–Si stretching was caused by the low amounts of oxygen located on the edge of the Si_6H_6. The FTIR spectra of Si_6H_6/*n*Li composites showed that the intensity of Si–OH, Si–O–Si, and Si–H stretching peaks decreased gradually, and a new broad absorption peak appeared at approximately 450 cm^{-1}. This new peak was also observed by the infrared microspectroscopic analysis of the low wavenumber region (Fig. S4) and can be assigned to the Si–Li stretching vibration mode based on *ab initio* molecular-dynamics calculation of the Si–Li mode structure (Fig. S5). FTIR measurements suggested that Si–OH, Si–O–Si, and Si–H groups react with Li by the mechanical milling process and that Si–Li bonds are formed on Si_6H_6.

The local environment of the silicon framework was examined by X-ray absorption near-edge structure (XANES) analysis. The Si K-edge absorption spectrum of Si_6H_6/*n*Li was compared to that of Si_6H_6 (Fig. 3C). Si_6H_6 showed a moderate spectral shape originating from 1836 eV and exhibited features at an energy of 1841 and 1847 eV. These peaks were at the same energy as that of the Si–Si bond in crystalline silicone terminated with hydrogen and layered polysilane.[13] Si_6H_6/*n*Li showed a shoulder peak at 1838 eV; thus, the XANES spectra shifted to a lower energy region compared to Si_6H_6. Furthermore, a new broad peak was observed at 1845 eV. The intensities of these new peaks increased due to the additive amounts of Li. These results indicated that the coordination environments of Si are changed by the mechanochemical reaction. The theoretical XANES spectra of Si–H and Si–Li structural models based on the FEFF program[21] also showed both a low energy shift of spectrum and the appearance of a new peak at a high energy region (Fig. 3D). This result also supports Si–Li bond formation in Si_6H_6/*n*Li. In addition, the Li K-edge XANES spectra of each composite suggest that Li exists as a cationic species (Li^+) in the composite (Fig. S6).

The XRD, FTIR, and XANES measurements indicated that the lithiation of Si_6H_6 proceeds and that a Si_6Li_6 composite is formed by

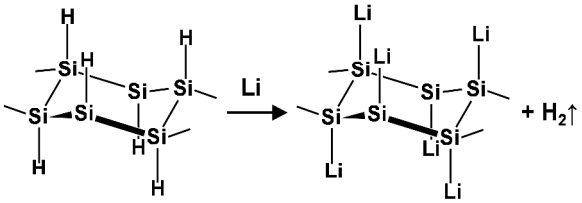

Scheme 1 Proposed reaction mechanism for formation of Si_6Li_6 by mechanochemical milling method

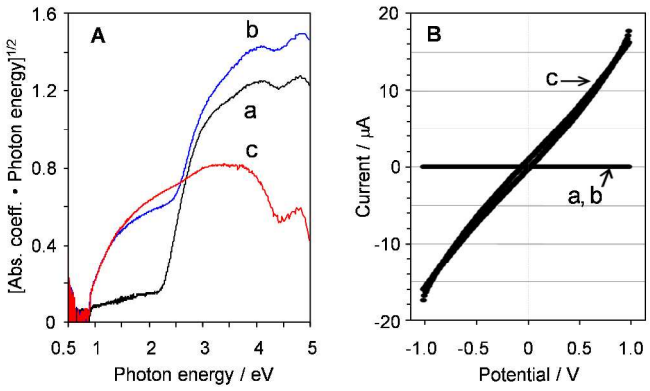

Fig. 4 Diffuse reflectance UV–vis spectra (A) and current–voltage (I–V) curves (B) of (a) Si_6H_6, (b) Si_6H_6/3Li, and (c) Si_6H_6/6Li

the mechanochemical solid-phase reaction of Si_6H_6 and equal amounts of Li against Si in Si_6H_6. The reaction mechanism is estimated to be a substitution of Si–H on the Si_6H_6 with Li, as is shown in Scheme 1. In this reaction, hydrogen gas is expected to be generated as a by-product simultaneous with the formation of the Si–Li bond. In fact, hydrogen gas was detected qualitatively from the periphery of the mortar during the mechanical milling of Si_6H_6 and Li by gas chromatography.

To investigate the changes in the electronic band structure due to the lithiation, solid-state diffuse reflectance UV–vis spectra were measured (Fig. 4A). Si_6H_6 showed a strong absorption band at the UV region with an edge at 576 nm, indicating that bandgap energy is 2.2 eV, which is in good agreement with previously published results.[22] On the other hand, the absorption band edge of Si_6Li_6 was shifted to a longer wavelength and showed lower bandgap energy (0.85 eV) than that of Si_6H_6. Si_6H_6/3Li showed that two absorption edges attributed to bandgaps of 0.85 and 2.2 eV, suggesting that both Si_6H_6 and Si_6Li_6-like moieties coexist in the composite due to the inhomogeneous distribution of Li in Si_6H_6/3Li. These results indicated that a new electron band level is formed by the lithiation of Si_6H_6.

To evaluate the conductive properties of the obtained composites, current–voltage (I–V) curves were measured at room temperature using a compressed disk of each composite (Fig. 4B). Si_6H_6 and Si_6H_6/3Li exhibited flat I–V curves resulting in insulating materials. Si_6Li_6 exhibited an ohmic I–V curve, although the observed current is quite low. The trend of conductive behaviors for each composite agreed with the changes in UV–vis spectrum. Consequently, both uniform lithiation and formation of the new electron band level are important to improve conductivity. In addition, the slope of I–V curve for Si_6Li_6 was significantly influenced by the preparation conditions of the composite or its compressed disk, suggesting that the grain boundary resistivity between Si_6Li_6 particles is greater than the internal resistance of the Si_6Li_6 particle.

The changes in the electronic band structure and the improvement of electron conductivity by the lithiation of polysilane are in agreement with predictions from a recent theoretical study.[17] Details of the conductive mechanism are under consideration; however, changes in the electronic band structure of the Si framework due to lithiation are estimated to be important relative to the conductive properties.

In this study, we have successfully prepared a new Si–Li composite, Si_6Li_6, by a mechanochemical solid-phase reaction of

Si_6H_6 and Li. The obtained Si_6Li_6 formed a Si–Li bond as a result of the substitution of Si–H with Li. Furthermore, the lithiation of polysilane led to changes in the electronic band structure and improved electron conductivity. The lithiation of Si_6H_6 described in this study has yielded important results for Li-ion batteries, ultrathin semiconductors, and energy conversion and storage devices. Further study using Si_6Li_6 as an anode material for Li-ion batteries is in progress.

This work was supported financially by the Japan Society for Promotion of Science, KAKENHI Grant-in-Aid for Young Scientists (B): No. 25871250 and the Japan Science and Technology Agency, Precursory Research for Embryonic Science and Technology. The work in the SR center was supported by "Project for Creation of Research Platforms and Sharing of Advanced Research Infrastructure". The synchrotron radiation experiments were performed on the BL43IR at SPring-8 with the approval of the Japan Synchrotron Radiation Research Institute, Proposal No. 2012B1965 and 2013A1341.

Notes and references

1 H. Wu and Y. Cui, *Nano Today*, 2012, **7** (5), 414–429.
2 U. Kasavajjula, C.S. Wang and A.J. Appleby, *J. Power Sources*, 2007, **163** (2), 1003–1039
3 A. Magasinski, P. Dixon, B. Hertzberg, A. Kvit, J. Ayala and G. Yushin, *Nature Materials*, 2010, **9**, 353–358.
4 T.D. Hatchard and J.R. Dahn, *J. Electrochem. Soc.*, 2004, **151**, A838–A842; B. Gao, S. Sinha, L. Fleming and O. Zhou, *Adv. Mater.*, 2001, **13**, 816–819.
5 T. Sasaki, M. Watanabe, H. Hashizume, H. Yamada and H. Nakazawa, *J. Am. Chem. Soc.*, 1996, **118**, 8329–8335; Y. Omomo, T. Sasaki, L. Wang and M. Watanabe, *J. Am. Chem. Soc.*, 2003, **125**, 3568–3575.
6 N. Miyamoto, H. Yamamoto, R. Kaito and K. Kuroda, *Chem. Commun.*, 2002, 2378–2379.
7 D. Yang, S.J. Sandoval, W.M.R. Divigalpitiya, J.C. Irwin and R.F. Frindt, *Phys. Rev. B*, 1991, **43**, 12053–12056.
8 G. Alberti, S. Cavalaglio, C. Dionigi and F. Marmottini, *Langmuir*, 2000, **16**, 7663–7668.
9 K.S. Novoselov, A.K. Geim, S.V. Morozov, D. Jiang, Y. Zhang, S.V. Dubonos, I.V. Grigorieva and A.A. Firsov, *Science*, 2005, **306**, 666–669; J.C. Meyer, A.K. Geim, M.I. Katsnelson, K.S. Novoselov, T.J. Booth and S. Roht, *Nature*, 2007, **446**, 60–63.
10 N.A. Kaskhedikar and J. Maier, *Adv. Mater.*, 2009, **21**, 2664–2680.
11 H. Nakano, M. Ishii and H. Nakamura, *Chem. Commun.*, 2005, 2945–2947.
12 H. Nakano, T. Mitsuoka, M. Harada, K. Horibuchi, H. Nozaki, N. Takahashi, T. Nonaka, Y. Seno and H. Nakamura, *Angew. Chem. Int. Ed.*, 2006, **45**, 6303–6306.
13 J. R. Dahn, B. M. Way, E. Fuller, *Phys. Rev B*, 1993, **48**, 17872–17877.
14 H. Okamoto, Y. Sugiyama and H. Nakano, *Chem. Eur. J.*, 2011, **17**, 9864–9887; H. Nakano, *J. Am. Chem. Soc.*, 2012, **134**, 5452–5455.
15 Y. Sugiyama, H. Okamoto, T. Mitsuoka, T. Morikawa, K. Nakanishi, T. Ohta and H. Nakano, *J. Am. Chem. Soc.*, 2010, **132**, 5946–5947; M.J.S. Spencer, T. Morishita, M. Mikami, I.K. Snook, Y. Sugiyama and H. Nakano, *Phys. Chem. Chem. Phys.*, 2011, **13**, 15418–15422.
16 H. Okamoto, Y. Kumai, Y. Sugiyama, T. Mitsuoka, K. Nakanishi, T. Ohta, H. Nozaki, S. Yamaguchi, S. Shirai and H. Nakano, *J. Am. Chem. Soc.*, 2010, **132**, 2710–2718.
17 V. V. Kulish, O. I. Malyi, M. F. Ng, Z. Chen, S. Manzhos and P. Wu, *Phys. Chem. Chem. Phys.*, 2014, **16**, 4260-4267.
18 W.J. Weydanz, M. Wohlfahrt-Mehrens and R.A. Huggins, *J. Power Sources*, 1999, **81**, 237–242.
19 R.A. Sharma and R.N. Seefurth, *J. Electrochem. Soc.*, 1976, **123**, 1763–1768.
20 S. Yamanaka, H. Matsu-ura and M. Ishikawa, *Mater. Res. Bull.*, 1996, **31**, 307–316.
21 A. L. Ankudinov, B. Ravel, J.J. Rehr and S.D. Conradson, *Phys. Rev. B*, 1998, **58**, 7565–7576.
22 K. Nishimura, Y. Nagano, S. Yamanaka and H. Matsu-ura, *Jpn. J. Appl. Phys.*, 1996, 35, L293–L296.

